Flight motor networks modulate primary olfactory processing in the moth *Manduca sexta*

Phillip D. Chapman[a,1], Rex Burkland[a,1], Samual P. Bradley[a], Benjamin Houot[a,2], Victoria Bullman[a], Andrew M. Dacks[a], and Kevin C. Daly[a,3]

[a]Department of Biology, West Virginia University, Morgantown, WV 26506

Edited by John G. Hildebrand, University of Arizona, Tucson, AZ, and approved April 11, 2018 (received for review December 23, 2017)

Nervous systems must distinguish sensory signals derived from an animal's own movements (reafference) from environmentally derived sources (exafference). To accomplish this, motor networks producing reafference transmit motor information, via a corollary discharge circuit (CDC), to affected sensory networks, modulating sensory function during behavior. While CDCs have been described in most sensory modalities, none have been observed projecting to an olfactory pathway. In moths, two mesothoracic to deutocerebral histaminergic neurons (MDHns) project from flight sensorimotor centers in the mesothoracic neuromere to the antennal lobe (AL), where they provide the sole source of histamine (HA), but whether they represent a CDC is unknown. We demonstrate that MDHn spiking activity is positively correlated with wing-motor output and increased before bouts of motor activity, suggesting that MDHns communicate global locomotor state, rather than providing a precisely timed motor copy. Within the AL, HA application sharpened entrainment of projection neuron responses to odor stimuli embedded within simulated wing-beat–induced flows, whereas MDHn axotomy or AL HA receptor (HA-r) blockade reduced entrainment. This finding is consistent with higher-order CDCs, as the MDHns enhanced rather than filtered entrainment of AL projection neurons. Finally, HA-r blockade increased odor detection and discrimination thresholds in behavior assays. These results establish MDHns as a CDC that modulates AL temporal resolution, enhancing odor-guided behavior. MDHns thus appear to represent a higher-order CDC to an insect olfactory pathway; this CDC's unique nature highlights the importance of motor-to-sensory signaling as a context-specific mechanism that fine-tunes sensory function.

corollary discharge | olfaction | antennal lobe | active sampling | ascending neuron

As animals locomote, their motor actions can directly affect sensory function, causing self-induced, or "reafferent," sensory neural responses. Unchecked, reafference can interfere with or otherwise influence the experience of externally derived or "exafferent" sensory cues. Furthermore, behaviors causing reafference can be an integral component of active sensory sampling strategies. For example, saccadic eye movements continually shift the retinal image in a ballistic fashion to interrogate the visual environment and yet visual experience is perceived as stable. This visual stabilization likely occurs because the superior colliculus sends information about eye-movement commands to the frontal eye field of the cortex (1). Such motor-to-sensory pathways are referred to as corollary discharge circuits (CDCs), which are a class of forward circuits that specifically provide information about motor activity to sensory systems, allowing them to account for behavior-induced effects on sensory function. CDCs can provide precisely timed facsimiles of motor commands (i.e., an efference copy) to modulatory-like signals that represent current or pending changes in behavioral state (2). While all CDCs provide motor information to sensory systems, they can be further classified based on their functional consequences on sensory processing. CDCs that filter out reafferent inputs or inhibit sensory-driven reflexes (e.g., refs. 3 and 4) are classified as lower-order CDCs, while those that predict, stabilize, facilitate sensory signal analysis, or sensory motor learning (e.g., refs. 5 and 6) can be classified as higher-order CDCs (2). Given their fundamental role in sensory-motor interactions, evidence of CDCs have been observed in vision (2, 5–7), hearing (4, 8, 9), and the sensing of body posture (10, 11), and their failure likely underlies sensory hallucinations in schizophrenia (12), Parkinson's disease (13), and dyspnea (14). Indeed, CDCs have been characterized to some degree in nearly every sensory domain except olfaction, and to date no higher-order CDC has been described in any invertebrate nervous system.

Like eye saccades in vertebrates, active olfactory sampling behaviors, such as sniffing, antennal and tongue flicking, and wing beating are periodic (15). These active sampling behaviors increase airflow and turbulence around the olfactory epithelium, inducing a mechanosensory component to olfactory neural responses observable even in the absence of odor (16–19). In the hawkmoth *Manduca sexta* and other related insects, wing beating, in addition to casting back and forth through odor plumes, is an important component of active odor-sampling behavior (20–22). Wing beating can generate substantial oscillatory airflow over the antennae (23) and vibrates the antennae at the frequency of the beating wing during flight (24). This implies that during odor-guided flight, olfactory sensory neurons on the antennae are periodically exposed to odorant molecules in higher

Significance

Across vertebrates and invertebrates, corollary discharge circuits (CDCs) project to and inform sensory networks about an animal's movements, which directly impact sensory processing. Failure of CDCs likely underlie sensory hallucinations in schizophrenia, Parkinson's disease, and dyspnea, highlighting the fundamental importance of CDCs for successfully interpreting sensory cues to adaptively interact with the external world. Ultimately, understanding the role of CDCs in integrating sensory motor function will be vital to understand these diseases, but mechanistically little is known about how CDCs function. CDCs have been identified in most sensory domains except olfaction. Our findings indicate that a histaminergic CDC enhances the ability of the olfactory system to more precisely encode stimulus temporal structure, resulting in enhanced olfactory acuity.

Author contributions: P.D.C., R.B., B.H., A.M.D., and K.C.D. designed research; P.D.C., R.B., S.P.B., B.H., and V.B. performed research; P.D.C., R.B., S.P.B., B.H., V.B., and K.C.D. analyzed data; and P.D.C., R.B., and K.C.D. wrote the paper.

The authors declare no conflict of interest.

This article is a PNAS Direct Submission.

[1]P.D.C. and R.B. contributed equally to this work.

[2]Present address: Division of Chemical Ecology, Department of Plant Protection Biology, Swedish University of Agricultural Sciences, S-230 53 Alnarp, Sweden.

[3]To whom correspondence should be addressed. Email: kevin.daly@mail.wvu.edu.

This article contains supporting information online at www.pnas.org/lookup/suppl/doi:10.1073/pnas.1722379115/-/DCSupplemental.

Published online May 7, 2018.

velocity flows induced by wing beating, presumably enhancing odor–receptor interactions (21). Far from hindering moths, periodic odor stimulation is readily tracked by both local interneurons (LNs) and projection neurons (PNs) of the antennal lobe (AL; the primary olfactory network) up to but not beyond ∼28 Hz, the maximum wing-beat frequency of this species (25). Pulsed delivery of odors elicits more distinctive AL odor representations relative to continuous odor stimulation (18), and appears to be required for several moth species to track and locate odor sources (20, 26, 27). In theory, the ability to track odors presented in the wing-beat frequency range could arise from purely feedforward mechanisms (28). However, AL neural tracking of stimuli presented across the wing-beat frequency range (0–28 Hz) requires neural connectivity between flight motor circuits in the thoracic neuromeres and the AL (25), suggesting that motor centers may directly influence the temporal resolution of the olfactory system. The only known connection between the flight-motor pattern-generating centers and the olfactory system in *M. sexta* is a single pair of mesothoracic to deutocerebral histaminergic (HA) neurons (MDHns); these cells represent the exclusive source of HA in the AL (29, 30). Within each AL of *M. sexta*, ∼16 predominantly GABAergic LNs express the HA-B receptor (MsHisClBr) and collectively these LNs ramify all AL glomeruli, whereas the HA-A receptor was not observed (30). In arthropods, there are only two known HA receptors (HA-r), both of which are fast inhibitory ionotropic Cl^- channels (31–33), suggesting that MDHns disinhibit the AL network when active.

Adult *M. sexta* primarily fly to locomote and use their legs to grasp objects that they land upon; this suggests that MDHn function primarily relates to flight behavior. Consistent with this, the MsHisClBr is not expressed within the larval antennal center (30), despite the MDHns being present and projecting to these centers across all larval stages. This implies that this circuit only becomes functional in adults and takes on a flight-related role. In most insects, the MDHns project to the subesophageal zone and antennal mechanosensory and motor center (AMMC). However, in nocturnally active plume-tracking insects, like caddisflies (34) and moths, the MDHns innervate the AL as well (35). Interestingly, this circuit appears to have been lost in closely related butterflies (35), which are diurnal and differ from moths in their flight mechanics and relative reliance on visual, rather than olfactory cues. The MDHns are therefore excellent candidates for a CDC between flight sensory motor centers in the ventral nerve cord and the olfactory system in the moth brain; however, neither their function during flight nor their functional role in olfactory processing and odor-guided behavior is known.

Here we demonstrate that the MDHns function as a higher-order, flight-to-olfactory CDC. We show that MDHn spiking activity is positively correlated to the ongoing level of wing-motor output and increased MDHn spike rate precedes bouts of motor output. Furthermore, increasing AL HA enhances entrainment to olfactory stimuli presented within the wing-beat frequency range, while disrupting AL HA-r function or removing MDHn input reduces entrainment. Finally, disruption of AL HA-r function decreases olfactory acuity in behavioral detection and discrimination threshold assays. Collectively, these results lead to the conclusion that during flight, the MDHns which likely disinhibit the AL network, up-regulate AL entrainment to the stimulus temporal structure, thereby enhancing olfactory acuity in behavioral assays. MDHns therefore do not filter the effects of wing-beat–induced sensory reafference from the neural response, as would be the case in a lower-order CDC. Rather, the MDHns up-regulate the ability of the olfactory system to entrain to the temporal features of the odor stimulus and enhance the ability of moths to both detect and discriminate between odors. Thus, these results appear to represent a higher-order motor-to-olfactory CDC.

Results

MDHn Activity Is Positively Correlated with Forewing Motor Output. The MDHns arborize throughout the dorsal aspect of the mesothoracic neuromere, which along with the metathoracic neuromere, house flight central pattern-generating circuitry, including wing sensory input (36–38). To characterize the relationship between the MDHns and wing-motor output, we developed an approach that leaves the entire central nervous system intact, exposing the mesothoracic neuromere where all sensory motor nerves emanating from the thoracic neuromeres were sectioned for stability; this also allowed us to make intracellular recordings from individual MDHns while simultaneously recording forewing depressor and elevator motor neuron output from the trunk IIN1b fiber using a suction electrode (39) (Fig. 1*A*). Intracellular electrode guidance to MDHns was visually blind, but spike shape and a tonic firing pattern guided selection of specific cells for recording. Each recorded cell was dye-filled, and HA-immunolabeling was used to confirm that an MDHn was recorded (Fig. 1*B*).

All recorded MDHns ($n = 5$) produced highly stereotyped spike waveforms and were tonically active even in the absence of motor output (Fig. 1*C*). In four of the five animals we were able to the hold intracellular recording long enough to induce wing-motor output via bath application of chlordimeform (10^{-5} M), an effective and selective octopamine agonist known to reliably induce fictive flight in insects, including *M. sexta* (36). In all cases MDHn tonic spike frequency was positively correlated with the presence and strength of wing-motor output (Fig. 1 *C*–*G*). This correlation could indicate that the MDHns receive input from motor circuitry or that chlordimeform directly affects the MDHns in parallel with motor circuitry. However, increases in MDHn firing rate were coupled to individual brief bouts of wing-motor output (Fig. 1*C*), suggesting that MDHn activity was coupled to motor output per se and not necessarily chlordimeform application. This also suggests that MDHns were driven by network components that produce and regulate the initiation and cessation of wing-motor output. In cases where wing-motor output increased or otherwise remained tonically active on a time scale of minutes, MDH activity increased in coordination with gradual increases in motor output (Fig. 1*D*). Mean normalized spike rate of both MDHn and IIN1b were positively correlated across all recordings (Fig. 1*E*) and manually segmenting recordings into epochs of wing-motor output versus "quiescence" (*SI Materials and Methods*) demonstrated a significant increase in MDHn spike rate during wing-motor output (Fig. 1*F*). Thus, the activity of MDHns represents a corollary of wing-motor output.

MDHn activity could provide two types of information about wing-motor output. MDHn spiking activity could be a precise efference copy of wing-motor function (indicative of a lower-order CDC), or rather than encoding precise wing movement, MDHn spiking activity could reflect the current behavioral state of the flight-motor network (observed in higher-order CDCs). Cross-correlation analysis revealed no temporally precise spiking relationships between the recorded motor-output fiber and MDHn (Fig. 1*G*). Rather, MDHn activity preceded bouts of motor activity by ∼100 ms and the correlation between MDHn and IIN1b spiking was only evident when data were smoothed across 25 ms or more (Fig. 1*G*), indicating that MDHn spiking activity and flight-motor output were correlated on a slower timescale. Thus, while MDHn and wing-motor output appear to be driven by an at least partially overlapping circuitry, the MDHns do not represent a precise efference copy per se. This is further supported by the observation that in all MDHn recordings, there was persistent tonic spiking in the absence of motor output. Thus, MDHns appear to encode changes in behavioral state.

AL Neural Entrainment to Stimulus Temporal Structure Is Modulated by Histamine. MHDns increase their spiking activity during wing-motor output, thus it stands to reason that HA release in the AL increases as well. We next asked whether HA release from the MDHns, which are the exclusive source of HA in the AL of *M. sexta* (30), affects neural responses to temporally patterned odor stimulation that simulates the periodic flow effects induced by wing beating (23). We therefore used extracellular tetrodes to

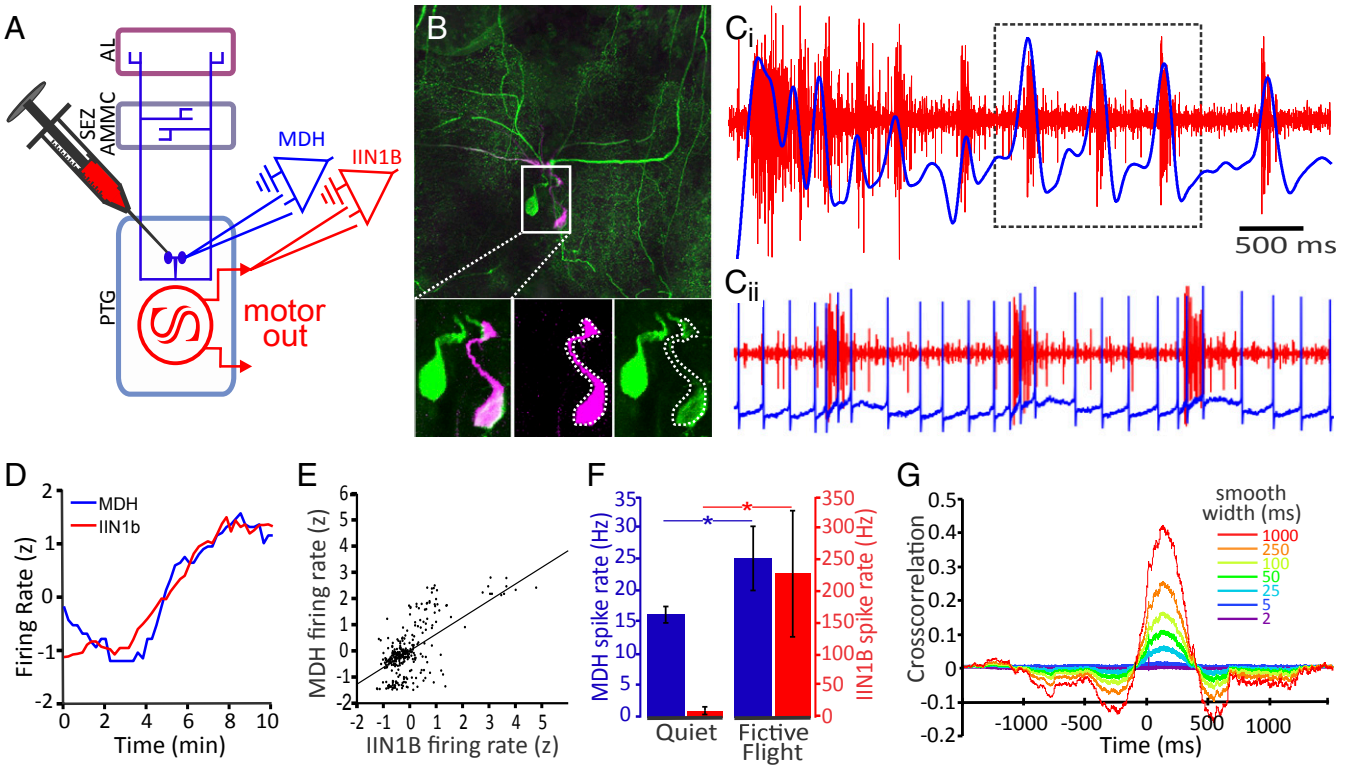

Fig. 1. MDH activity is correlated with flight-motor patterns. (*A*) Schematic of key components of the moth CNS, including the AL, subesophageal zone (SEZ), and AMMC and the pterothoracic ganglion (PTG), which includes the fused mesothoracic and metathoracic neuromeres. Also highlighted is our experimental approach, which included the simultaneous intracellular recording of an MDHn (blue) and suction electrode recording of the IIN1b nerve fiber (red), while wing-motor output is driven from the flight central pattern generator (red circle) via bath-applied chlordimeform (50 μM). (*B*) HA immunolabeling (green) of the MDHns with the intracellularly recorded MDHn filled with Alexa 568 (magenta; magnification = 20×). *Inset* below is a zoom-in of two distinct cell bodies labeled. (*Left*) Both laser channels. (*Center*) Alexa 568 channel showing a single filled cell body and primary neurite. (*Right*) HA channel showing the two cell bodies and primary neurites of the MDHn pair. Complete spatial overlap confirms the recording was of a MDHn. (C_i) Superimposition of the smoothed instantaneous spike rate of the recorded MDHn (blue) and the raw extracellular recording of the IIN1b fiber (red). Dashed rectangle highlights the time sample shown in C_{ii}, which shows the raw spike trains for both traces. Note that the MDH spike rate always increases just before and during bouts of wing motor output. (*D*) Plot of *z*-score normalized spike rate for MDH (blue) and IIN1b (red) across 10 min of continuous recording, demonstrating that as IIN1b activity increases over time, so too does MDH spike rate ($r = 0.71$). (*E*) Scatterplot of *z*-score normalized spike rate of MDH and IIN1b. Linear regression ($n = 4$ recordings/738 points; $R^2 = 0.09$, $r = 0.30$). (*F*) Mean spike rate from epochs where the IIN1b was quiet versus producing wing-motor output from the recording highlighted in *C*. Error bars represent the SE. Statistical comparisons between states indicates corresponding significant increase in both IIN1b and MDH (Welch's *t* test; $n = 8$ recording segments; $^*P < 0.05$). (*G*) Cross-correlation between MDH and IIN1b firing rates using Gaussian smoothing windows ranging in width from 2 ms to 1,000 ms. Note that for smoothing widows within typical spike integration times (2–5 ms), there is no correlation between measures.

record simultaneously from multiple individual AL neural units (40) while stimulating the antenna with a single odorant (either 2-hexanone or 2-octanone). Odor was presented in blocks of five 500-ms-long 20-Hz pulse trains using a 50% duty cycle (i.e., 25-ms on and 25-ms off) and 10 s between each train of a block. This was repeated every 2 min for 30 min. After the first block, the moth received one of the three treatments (Fig. 2*A*). On average 18–22% of AL neural units within each group entrained to odor pulse trains. Based on their spiking characteristics, these units can be putatively classified as PNs (41). First, to disrupt HA function, we bath-applied the HA-r antagonist cimetidine (500 μM) (Fig. 2*A*). In many units that were initially able to entrain to 20-Hz pulsed stimuli, cimetidine application decreased their ability to entrain to stimulus temporal structure. For example, the unit depicted in Fig. 2*B* initially responded reliably to all 10 pulses of the pulse train across all five repeats, as indicated by 10 prominent peaks in the histogram. After cimetidine application, the same unit failed to reliably entrain to the stimulus; it failed to respond to the first two pulses then consistently responded to three, perhaps four subsequent pulses. To evaluate the ability of units to entrain to the 20-Hz pulse trains, we calculated power spectral densities for each unit in response to each stimulus block, then calculated the integrated power from 18 to 22 Hz (25). Cimetidine application significantly decreased the mean integrated power across units over time indicating that, relative to time matched controls, the ability of units to entrain to pulsed odor had degraded within 6 min of application (Fig. 2*C*). If blocking HA-r function reduces the ability of AL neurons to entrain to pulsed stimuli, it stands to reason that removing input from the sole source of HA in the AL (the MDHns) (30) should have the same effect. Therefore, our second approach was to sever the neck connective in a second group of moths, thus axotomizing the two MDHn axons therein (Fig. 2*A*). As with cimetidine application, we observed that in moths where the neck connectives were cut, units that were initially able to reliably track pulsed odor were less able to track over time relative to time-matched sham surgery controls (e.g., Fig. 2*D*). Across the population this manifests as a significant reduction in integrated power around the pulsing frequency within 16 min (Fig. 2*E*). It is important to note that entrainment across the population was not completely lost in either case. Rather, there was a loss of responses to individual pulses of a train (Fig. 2*B*, red box) and the relative degradation in ability of the cell to produce discrete bursts to individual pulses separated by interstitials with no spiking (Fig. 2*D*, before vs. after). Finally, if disrupting the MDH circuit degrades the temporal fidelity of odor encoding, bath application of HA should have the opposite effect. Therefore, in a final group of moths HA (50 μM) was

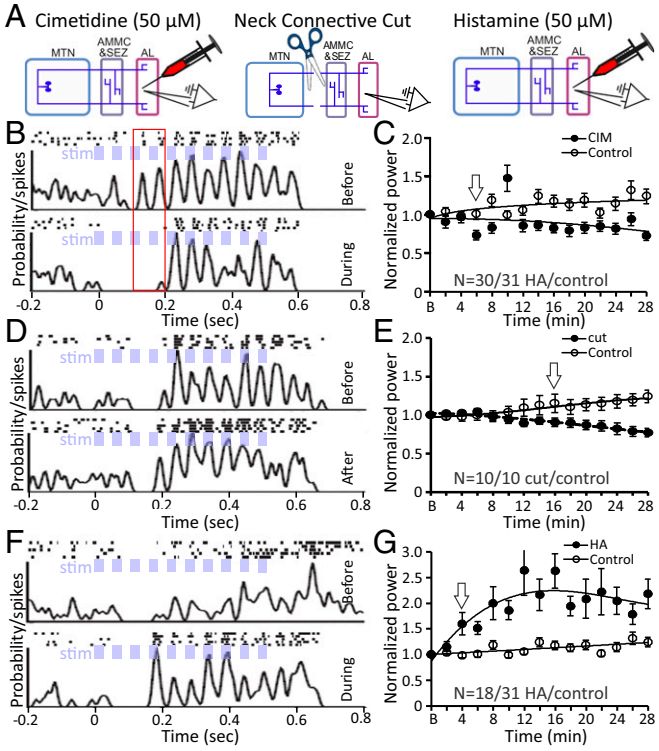

Fig. 2. HA enhances entrainment of AL PNs to rapidly pulsed odor. (*A*) To evaluate the effect of MDHn HA release on the ability of AL PNs to entrain to pulsed stimuli, we performed three experiments, each in separate groups of animals. For all experiments, multichannel electrodes were placed into the AL and multiunit recordings were made while the ipsilateral antenna was stimulated with a block of five 500-ms-long stimulation at 20-Hz pulse trains every 2 min for a total of 15 presentations. After the first block of pulse trains, animals were challenged with an experimental treatment. (*Left*) In the first experiment, to disrupt HA-r function we bath-applied 50 μM cimetidine (CIM) in saline vehicle continuously over the course of the experiment. (*Center*) In the second experiment of animals, to remove intrinsic HA input from the MDHns the neck connective was cut, thereby axotomizing the MDHns. (*Right*) In the third experiment of animals, direct bath application of HA (50 μM) in saline vehicle was used to simulate increased MDHn output during flight. Exemplar peristimulus rasters and histograms for the baseline responses (before) and during/after cimetidine (*B*), neck connective cut (*D*), and HA (*F*) treatments. Mean integrated power from 18 to 22 Hz by time across all recorded neurons that entrained to the pulsed odor at some point during cimetidine (*C*), neck connective cut (*E*), and HA (*G*) treatments. Error bars represent the SE. Results plotted as a function of time since treatment. Power was normalized by dividing mean power from each block by the mean baseline (pretreatment block) power. Arrows indicated the first block where there was a significant difference in power between experimental and control treatments (Welch's *t* test for two samples with unequal variance; $P < 0.05$). Regressions are second order polynomials. Red rectangle (*B*) highlights the loss of responses to the first two pulses as a consequence of cimetidine relative to pretreatment.

bath-applied during pulsed odor stimulation (Fig. 2*A*). Within 4 min of initiating HA application, the ability of individual units within the ensemble to entrain to the stimulus temporal structure increased, and in some instances units that did not initially entrain to odor pulses were recruited into the population of entrained units (e.g., Fig. 2*F*). Across the population, we observed a significant increase in mean integrated power at the pulsing frequency relative to controls (Fig. 2*G*). This HA-induced increase in power only occurs at the pulse frequency and does so as the overall population spiking response to the pulse trains increases as well (Fig. S1). These results collectively indicate that MDHn release of HA within the AL enhances entrainment to the stimulus temporal structure as opposed to filtering out the reafference. This again supports the notion that this circuit be classified as a higher-order CDC (2).

Olfactory Acuity Is Histamine Dependent. The capacity for the olfactory system to guide behavior is fundamentally dependent on its ability to detect and identify (i.e., discriminate) important odors. Simulating wing-beat–induced flows enhances both separation of neural representations of different odors (18) and olfactory acuity in behavioral assays (25, 42). Therefore, we predict that because this CDC enhances odor processing, it will likewise enhance behavioral measures of odor detection and discrimination. Two behavioral assays were used to determine if HA circuit function contributes to the detection and discrimination of odors (*SI Materials and Methods*). Both assays were based on a well-established Pavlovian olfactory learning approach (43–48), where moths were first conditioned (for detection assays) or differentially conditioned (for discrimination assays) to respond to target odors. Twenty-four hours post-conditioning, moths were randomly assigned into drug or control injection treatments and tested in a blind format. Based on initial control experiments (Fig. S2), an effective dose of ∼1 nL of 50 μM cimetidine was injected into each AL. Fifteen minutes following injection, moths were challenged with a blank stimulus, then a series of increasing concentrations of the conditioned odor to determine the concentration at which they detected the odor as measured by a significant increase in conditioned feeding response relative to the response to blanks. Both groups acquired the conditioned response (Fig. 3*A*). However, tests subsequent to injection indicated that cimetidine-injected moths displayed an order-of-magnitude higher detection threshold relative to controls (Fig. 3*B*). This was replicated using a different HA-r antagonist, ranitidine (*SI Materials and Methods*, *SI Behavioral Results*, and Fig. S3). Collectively, these results suggest that HA within the AL enhances olfactory sensitivity.

As detection is a prerequisite for identification (44, 47), it stands to reason that increased detection thresholds would also impact the moths ability to identify target odors. Here we observed that discrimination thresholds also increased when HA-r function was blocked. Moths in both drug-treated and control groups learned to differentially respond to the CS^+ (odor paired with 0.75 M sucrose solution) and CS^- (odor only) odors (Fig. 3*C*). Again, 24 h after conditioning, moths were injected with either cimetidine or the saline vehicle, this time in a double-blind format. We then tested with both the CS^+ and CS^- odors across a dilution series of increasing concentration to determine the odor discrimination threshold, the lowest odor concentration at which moths responded significantly more to the CS^+ relative to the CS^- (i.e., a "conditioned differential response") (*SI Materials and Methods*). The discrimination threshold for saline-injected moths occurred at an odor concentration of 0.1 μg/2 μL, but when injected with cimetidine, a significant differential response was observed at 10.0 μg/2 μL. Thus, disruption of HA-r function decreases both the ability to detect (Fig. 3*B*) and identify (Fig. 3*D*) odors.

Discussion

Nervous systems must coordinate sensory with motor network function to adjust sensory processing based on planned and ongoing motor activities. CDCs are one class of neural circuits that provide information about motor output to sensory pathways to optimize sensory processing within the context of specific behaviors. CDCs can be broadly classified into two categories—lower-order and higher-order—defined based on the functional consequence they have on their target sensory pathway (2). Lower-order CDCs directly inhibit the reafference with precisely timed spikes that gate sensory signals (4). Higher-order CDCs on the other hand, can activate hundreds of milliseconds before the onset of a behavior and can modulate the state of a sensory network to accommodate imminent changes in behavior (9). Furthermore, higher-order CDCs do not block or filter the reafferent sensory input; rather, they exploit the reafferent input to facilitate sensory processing (2). Several studies in insects have

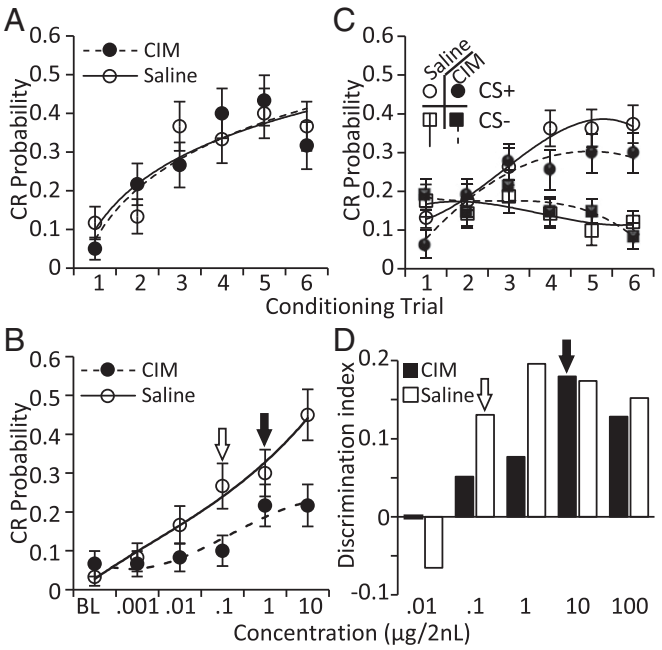

Fig. 3. HA-r blockade disrupts behavioral measures of olfactory acuity. (*A*) Acquisition of the conditioned feeding response to a single odor (2-hexanone) as a function of conditioning trial for groups of moths in the detection threshold assay. Twenty-four hours later, one group of moths was bilaterally injected with either 50 μM cimetidine (CIM) in saline vehicle or the saline vehicle without drug (saline) in a blind manner, then tested. (*B*) Conditioned feeding response as a function of odor concentration for the CIM and saline groups. Open and filled arrowheads indicate detection threshold concentrations, for the saline and CIM groups, respectively, as defined by the lowest concentration odor yielding a significant increase in response relative to the blank (one-tailed paired *t* test; $n = 60$; $P < 0.001$). (*C*) Acquisition of the differential conditioned feeding response to the CS^+ and CS^- stimuli for CIM- and saline-injected groups. Moths were first differentially conditioned to one of the two odorants (2-hexanone or 2-octanone). Both odors were used as the CS^+ and CS^- in separate but equally sized groups to counterbalance odor-dependent effects; for display, data were pooled by CS^+ and CS^-. (*D*) Discrimination index $[(CS^-) - (CS^+)]$ displayed by concentration for the CIM- and saline-injected groups. Open and filled arrowheads indicate discrimination threshold, the concentration at which there was a significant differential response to the CS^+ and CS^- odors using a one-tailed paired *t* tests (saline controls: $P = 0.03$; $n = 46$; CIM injected: $P = 0.05$; $n = 43$). All Regression lines are third-order polynomials and all error bars represent the SE.

characterized different neural circuit mechanisms that coordinate modulation of sensory processing with changes in behavioral state, such as flight- or walking-triggered release of octopamine to modulate processing of visual flow (49–51). Our results indicate that the MDHns are a higher-order CDC that function to disinhibit the AL in advance of imminent motor actions of the wings, enhancing the ability of the AL to entrain to the stimulus temporal structure. MDHn firing rate increases just before and during wing-motor output, but is not synchronous with IIN1b motor neuron spiking, suggesting that the MDHns do not provide precise information about the timing of motor output (i.e., an efference copy), but rather they appear to represent the broad behavioral state of flight.

The input signals that drive MDHn activity remain unknown, although the list of candidates is relatively small and includes: sensory afferents from the wings, legs, and thorax; central neurons that mediate motor patterns; and the motor neurons themselves. Sensory afferents are unlikely to drive MDHns as our approach was to cut all thoracic sensory afferent (and motor) fibers; this occurred ∼45 min before recording. Furthermore, in *M. sexta*, MDHn local processes within the mesothoracic neuromere are restricted to its dorsomedial aspect (30), while sensory afferents in a closely related moth species predominately innervate its ventrolateral aspect (38). However, we cannot rule out the possibility that sensory input to the pterothoracic ganglia normally contributes to MDHn activity in intact animals. Additionally, MDHn activity precedes wing-motor output, making it unlikely that motor output drives their activity either. Thus, our anatomical and physiological data suggest that these cells are centrally (as opposed to peripherally) driven.

The ability of the olfactory system to track odor timing is highly dependent on LNs that control a variety of network-wide coding features, including the transient nature of PN responses (52, 53). LNs therefore represent an elegant target for CDCs to regulate a sensory network. Pulse tracking is only weakly present in antennal field recordings in *M. sexta* but dominates AL local field potentials and spiking in at least some PNs. Furthermore, pulse tracking is both odor- and GABA-dependent, which implies lateral interactions clarify this periodic signal (25). Thus, while GABA mediates pulse tracking in PNs, our current results suggest that the MDHns modulate this ability, and that LNs are the most likely target. Indeed, arthropods express just two HA-rs, both of which are ionotropic Cl^- channels (31–33) and the AL of *M. sexta*; the MsHisClB receptor is expressed exclusively by ∼16 GABAergic AL LNs, which broadly ramify the entire AL (30). This implies that during flight, increased MDHn activity inhibits this subpopulation of inhibitory LNs. While the postsynaptic targets of these 16 LNs are unknown, the consequence of HA signaling is enhancement of the AL network to encode the temporal structure of olfactory stimuli at the level of PN output. This in turn enhances detection and identification at the level of sensory perception. Given that mammalian sniffing behavior produces the same physical flow effects as wing beating, it stands to reason that an analogous system might facilitate olfaction in mammals, although we cannot rule out the possibility that this CDC might also function to generally increase frequency response to the relatively more rapid stimulus temporal structure encountered during upwind flight.

If the MDHns sharpen AL entrainment to pulsed stimuli, how might this result in enhanced behavioral performance in the psychophysical assays of olfactory sensitivity and acuity? Primary olfactory networks are spontaneously active and noisy. Superimposed upon olfactory network dynamics are weak mechanosensory-driven oscillatory dynamics produced by active sampling behaviors, like sniffing (16, 17) and wing beating (23, 24). While AL neurons can be entrained to pulses of clean air (18, 25), moths do not respond to these clean-air pulse trains in behavioral assays (relative to the same duration continuous clean-air stimulus), and thus oscillating mechanosensory responses from the AL are behaviorally subthreshold. However, pulsed odor stimuli are more easily detected in behavioral detection threshold assays than continuous stimuli (25, 42), suggesting that antennal and AL mechanosensory responses, which are time-coupled and summate with odor-evoked activity, may facilitate stronger odor responses. Our results suggest that the MDHns fine-tune AL entrainment to oscillating airflow while the moth is in flight and actively seeking odor sources, rather than canceling out these weak mechanosensory oscillations, as would be the case for a lower-order CDC.

Taking these data together, we demonstrate that the MDHns represent an olfactory CDC that enhances olfactory processing presumably during flight. The MDHns interconnect flight motor centers and the olfactory system and are active during wing-motor output, which results in enhanced the temporal fidelity of AL neurons and odor-guided behavior of moths. Thus, the MDHns meet the criteria of a CDC. Furthermore, the MDHns appear to function as a higher-order CDC to the AL as their activity sharpens temporal entrainment to the stimulus. Thus, the MDHns likely influence the ability of the AL network to track odor timing and facilitate assembly of a salient "olfactory image." Given that odor-guided behavior in *M. sexta* is performed primarily during flight and the MDHns originate in a flight sensory

and motor pattern-generating center, we propose that the MDHns optimize olfactory function within the context of odor-guided flight. Finally, given their ubiquity across insects (35) and their projections into multiple additional sensory processing centers, we have only begun to understand the multimodal nature of MDHn's role in coordinating wing-motor actions with sensory processing.

Materials and Methods

SI Materials and Methods detail all experimental procedures. Briefly, intracellular recordings of MDHns were made in "CNS intact" preparations that exposes the pterothoracic ganglion and lesions-only nerves emanating from the pro-, meso-, and metathoracic neuromeres to eliminate muscle contraction near the recording site. Multiunit studies of AL neural spiking responses to pulsatile stimuli were performed using a fully intact preparation described in ref. 48. Putative PNs are identified on spiking characteristics (41). Equal ratios of males and females were used for all behavior pharmacology experiments. All behavioral pharmacological methods and psychophysical assays have been previously detailed (44, 46, 47).

ACKNOWLEDGMENTS. We thank Mark Willis for fruitful discussions during the course of this research and Sadie Bergeron and Gary Marsat for comments on this manuscript. This research was supported by NIH Grant DC009417 (to K.C.D.) and Air Force Office of Scientific Research Grant FA9550-17-1-0117 (to K.C.D. and A.M.D.).

1. Sommer MA, Wurtz RH (2008) Visual perception and corollary discharge. *Perception* 37:408–418.
2. Crapse TB, Sommer MA (2008) Corollary discharge across the animal kingdom. *Nat Rev Neurosci* 9:587–600.
3. Roy JE, Cullen KE (2004) Dissociating self-generated from passively applied head motion: Neural mechanisms in the vestibular nuclei. *J Neurosci* 24:2102–2111.
4. Poulet JF, Hedwig B (2002) A corollary discharge maintains auditory sensitivity during sound production. *Nature* 418:872–876.
5. Sommer MA, Wurtz RH (2006) Influence of the thalamus on spatial visual processing in frontal cortex. *Nature* 444:374–377.
6. Cavanaugh J, Berman RA, Joiner WM, Wurtz RH (2016) Saccadic corollary discharge underlies stable visual perception. *J Neurosci* 36:31–42.
7. Rath-Wilson K, Guitton D (2015) Oculomotor control after hemidecortication: A single hemisphere encodes corollary discharges for bilateral saccades. *Cortex* 63:232–249.
8. Poulet JFA, Hedwig B (2006) The cellular basis of a corollary discharge. *Science* 311: 518–522.
9. Schneider DM, Nelson A, Mooney R (2014) A synaptic and circuit basis for corollary discharge in the auditory cortex. *Nature* 513:189–194.
10. Montgomery JC, Bodznick D (1994) An adaptive filter that cancels self-induced noise in the electrosensory and lateral line mechanosensory systems of fish. *Neurosci Lett* 174:145–148.
11. Moore JD, et al. (2013) Hierarchy of orofacial rhythms revealed through whisking and breathing. *Nature* 497:205–210.
12. Ford JM, et al. (2013) Neurophysiological evidence of corollary discharge function during vocalization in psychotic patients and their nonpsychotic first-degree relatives. *Schizophr Bull* 39:1272–1280.
13. Brown P (2003) Oscillatory nature of human basal ganglia activity: Relationship to the pathophysiology of Parkinson's disease. *Mov Disord* 18:357–363.
14. Meek PM, et al.; American Thoracic Society (1999) Dyspnea. Mechanisms, assessment, and management: A consensus statement. *Am J Respir Crit Care Med* 159:321–340.
15. Halpern BP (1983) Tasting and smelling as active, exploratory sensory processes. *Am J Otolaryngol* 4:246–249.
16. Walsh RR (1956) Single cell spike activity in the olfactory bulb. *Am J Physiol* 186: 255–257.
17. Macrides F, Chorover SL (1972) Olfactory bulb units: Activity correlated with inhalation cycles and odor quality. *Science* 175:84–87.
18. Houot B, Burkland R, Tripathy S, Daly KC (2014) Antennal lobe representations are optimized when olfactory stimuli are periodically structured to simulate natural wing beat effects. *Front Cell Neurosci* 8:159.
19. Connelly T, et al. (2015) G protein-coupled odorant receptors underlie mechanosensitivity in mammalian olfactory sensory neurons. *Proc Natl Acad Sci USA* 112: 590–595.
20. Obara Y (1979) Bombyx mori mationg dance: An essential in locationg the female. *Appl Entomol Zool* 14:130–132.
21. Loudon C, Koehl MA (2000) Sniffing by a silkworm moth: Wing fanning enhances air penetration through and pheromone interception by antennae. *J Exp Biol* 203: 2977–2990.
22. Bau J, Justus KA, Cardé RT (2002) Antennal resolution of pulsed pheromone plumes in three moth species. *J Insect Physiol* 48:433–442.
23. Sane SP, Jacobson NP (2006) Induced airflow in flying insects II. Measurement of induced flow. *J Exp Biol* 209:43–56.
24. Sane SP, Dieudonné A, Willis MA, Daniel TL (2007) Antennal mechanosensors mediate flight control in moths. *Science* 315:863–866.
25. Tripathy SJ, et al. (2010) Odors pulsed at wing beat frequencies are tracked by primary olfactory networks and enhance odor detectio. *Front Cell Neurosci* 4:1–14.
26. Baker TC, Willis MA, Haynes KF, Phelan PL (1985) A pulsed cloud of sex pheromone elicits upwind flight in male moths. *Physiol Entomol* 10:257–265.
27. Willis MA, Baker TC (1984) Effects of intermittent and continuous pheromone stimulation on the flight behaviour of the oriental fruit moth, *Grapholita molesta*. *Physiol Entomol* 9:341–358.
28. Szyszka P, Gerkin RC, Galizia CG, Smith BH (2014) High-speed odor transduction and pulse tracking by insect olfactory receptor neurons. *Proc Natl Acad Sci USA* 111: 16925–16930.
29. Homberg U (1994) *Distribution of Neurotransmitters in the Insect Brain*, Progress in Zoology (Gustav Fischer, Stuttgart, Germany) Vol 40.
30. Bradley SP, Chapman PD, Lizbinski KM, Daly KC, Dacks AM (2016) A flight sensory-motor to olfactory processing circuit in the moth Manduca sexta. *Front Neural Circuits* 10:5.
31. Hardie RC (1988) Effects of antagonists on putative histamine receptors in the first visual neuropile of the housefly (*Musca domestica*). *J Exp Biol* 138:221–241.
32. Hardie RC (1989) A histamine-activated chloride channel involved in neurotransmission at a photoreceptor synapse. *Nature* 339:704–706.
33. Roeder T (2003) Metabotropic histamine receptors—Nothing for invertebrates? *Eur J Pharmacol* 466:85–90.
34. Löfstedt C, Hansson BS, Petersson E, Valeur P, Richards A (1994) Pheromonal secretions from glands on the 5th abdominal sternite of hydropsychid and rhyacophilid caddisflies (Trichoptera). *J Chem Ecol* 20:153–170.
35. Chapman PD, et al. (2017) Co-option of a motor-to-sensory histaminergic circuit correlates with insect flight biomechanics. *Proc Biol Sci* 284:20170339.
36. Kinnamon SC, Klaassen LW, Kammer AE, Claassen D (1984) Octopamine and chlordimeform enhance sensory responsiveness and production of the flight motor pattern in developing and adult moths. *J Neurobiol* 15:283–293.
37. Vierk R, Pflueger HJ, Duch C (2009) Differential effects of octopamine and tyramine on the central pattern generator for Manduca flight. *J Comp Physiol A Neuroethol Sens Neural Behav Physiol* 195:265–277.
38. Ando N, Wang H, Shirai K, Kiguchi K, Kanzaki R (2011) Central projections of the wing afferents in the hawkmoth, *Agrius convolvuli*. *J Insect Physiol* 57:1518–1536.
39. Eaton JL (1974) Nervous system of the head and thorax of the adult tobacco hornworm, *Manduca sexta* (Lepidoptera: Sphingidae). *Int J Insect Morphol Embryol* 3: 47–66.
40. Daly KC, Wright GA, Smith BH (2004) Molecular features of odorants systematically influence slow temporal responses across clusters of coordinated antennal lobe units in the moth *Manduca sexta*. *J Neurophysiol* 92:236–254.
41. Lei H, Reisenman CE, Wilson CH, Gabbur P, Hildebrand JG (2011) Spiking patterns and their functional implications in the antennal lobe of the tobacco hornworm *Manduca sexta*. *PLoS One* 6:e23382.
42. Daly KC, Kalwar F, Hatfield M, Staudacher E, Bradley SP (2013) Odor detection in *Manduca sexta* is optimized when odor stimuli are pulsed at a frequency matching the wing beat during flight. *PLoS One* 8:e81863.
43. Daly KC, Smith BH (2000) Associative olfactory learning in the moth Manduca sexta. *J Exp Biol* 203:2025–2038.
44. Daly KC, Carrell LA, Mwilaria E (2008) Characterizing psychophysical measures of discrimination thresholds and the effects of concentration on discrimination learning in the moth *Manduca sexta*. *Chem Senses* 33:95–106.
45. Daly KC, et al. (2016) Space takes time: Concentration dependent output codes from primary olfactory networks rapidly provide additional information at defined discrimination thresholds. *Front Cell Neurosci* 9:515.
46. Daly KC, Carrell LA, Mwilaria E (2007) Detection versus perception: Physiological and behavioral analysis of olfactory sensitivity in the moth (*Manduca sexta*). *Behav Neurosci* 121:794–807.
47. Mwilaria EK, Ghatak C, Daly KC (2008) Disruption of GABAA in the insect antennal lobe generally increases odor detection and discrimination thresholds. *Chem Senses* 33:267–281.
48. Daly KC, Christensen TA, Lei H, Smith BH, Hildebrand JG (2004) Learning modulates the ensemble representations for odors in primary olfactory networks. *Proc Natl Acad Sci USA* 101:10476–10481.
49. van Breugel F, Dickinson MH (2014) Plume-tracking behavior of flying *Drosophila* emerges from a set of distinct sensory-motor reflexes. *Curr Biol* 24:274–286.
50. Suver MP, Mamiya A, Dickinson MH (2012) Octopamine neurons mediate flight-induced modulation of visual processing in *Drosophila*. *Curr Biol* 22:2294–2302.
51. Lüders J, Kurtz R (2015) Octopaminergic modulation of temporal frequency tuning of a fly visual motion-sensitive neuron depends on adaptation level. *Front Integr Nuerosci* 9:36.
52. Christensen TA, Waldrop BR, Hildebrand JG (1998) Multitasking in the olfactory system: Context-dependent responses to odors reveal dual GABA-regulated coding mechanisms in single olfactory projection neurons. *J Neurosci* 18:5999–6008.
53. Christensen TA, Waldrop BR, Harrow ID, Hildebrand JG (1993) Local interneurons and information-processing in the olfactory glomeruli of the moth *Manduca sexta*. *J Comp Physiol A* 173:385–399.